LAWRENCE
LIVERMORE
NATIONAL
LABORATORY

LLNL-JRNL-414197

Fractal Growth in Organic Thin Films: Experiments and Modeling

G. Zhang, B. Reed, R. Gee, A. Maiti

June 25, 2009

Applied Physics Letters

Disclaimer

Fractal Growth in Organic Thin Films: Experiments and Modeling

Gengxin Zhang, Brandon Weeks *[a]

Chemical Engineering Department, Texas Tech University, Lubbock, TX79409, USA

Richard Gee, Amitesh Maiti *[b]

Lawrence Livermore National Laboratory, University of California, Livermore, CA 94451

*Corresponding author: a) Brandon.weeks@ttu.edu , b) amaiti@llnl.gov

Abstract

Optical Microscopy and Atomic Force Microscopy (AFM) were used to investigate the solidification process of the organic energetic material pentaerythritol tetranitrate (PETN) thermally deposited on a silicon surface. The metastable films spontaneously undergo dendrite formation where the measured fractal dimensions indicate a diffusion-limited-aggregation mechanism. The branch growth rate was investigated as a function of temperature and fitted by a theoretical model that takes into account competing thermally activated processes of surface diffusion and molecular desorption. Consideration of the internal molecular degrees of freedom is shown to be essential for quantitative consistency between theory and experiment.

Keywords: Dendritic growth, Diffusion-limited aggregation, Organic thin films

The physics of thin organic film growth is an intriguing and important topic in non-equilibrium solidification process.[1,2] Examples of such processes include non-equilibrium pattern formation[3], dendrite growth[2], and viscous fingering.[4] A number of growth and aggregation models have been developed to explain the physical and chemical characteristics including: diffusion limited aggregation (DLA),[5] cluster-cluster aggregation (CCA),[6] and deposition diffusion and aggregation (DDA)[7]. These models have been used for both metal[8, 9] and inorganic[10] thin films. The majority of studies have considered metallic systems where aggregation and desorption involve individual metal atoms. Expanding these models to a molecular system would be interesting due to the additional internal degrees of freedom of individual molecules that strongly affect kinetics. In addition, molecular thin films are important in many areas including pharmaceuticals,[11] paints/pigments, agrochemicals,[12] and energetic materials.[13]

In this letter, we report the investigation of fractal growth of pentaerythritol tetranitrate (PETN) films thermally deposited on a silicon substrate. At room temperature, the island growth clearly exhibits dendrite shapes with fractal dimensions typical of a DLA process. We develop a simple theoretical model to show how such patterns can be explained on the basis of competing effects of diffusion-mediated aggregation and desorption of molecules.

PETN (purity > 99%) supplied by Lawrence Livermore National Laboratory (LLNL) was used in these experiments without further purification. Electronic-grade silicon wafers (Nova Electronic Materials Ltd.) were cleaned by a routine procedure.[14] PETN films were deposited with thermal deposition chamber[15], which has *in situ* temperature and thickness measurement capability. An QCM Maxtek T-100 film thickness monitor

was used to check the flux and film thickness. The as-deposited PETN films, ranged from 10 to 1000 nm in thickness, were annealed at temperatures ranging from 30 ºC and 80 ºC, while the film growth process was monitored by optical microscopy. All atomic force microscopy (AFM) images were collected using a Nanoscope IIIa multimode scanning probe microscope (Veeco Instruments Inc., Santa Barbara, CA) operating in the tapping mode using a silicon cantilever with a nominal drive frequency of 325 kHz.

AFM images of the freshly prepared PETN films appear to follow the Volmer-Weber structure[16] with island structures as shown in Figure 1. PETN is easily super-cooled to room temperature without crystallization (melting point 141 ± 1°C[17]). The nucleation rate of islands appears to be homogeneous over the entire surface. The initial films prepared are metastable over a period of days showing no dendritic growth. Previous studies showed that by inducing defects on the surface with the AFM tip, PETN films spontaneously undergo dendritic formation.[18] However, that work was primarily phenomenological and there was no effort to deduce the mechanisms responsible for the fractal growth. Figure 2 shows clear observation of branch-formation at four subsequent time elapses after initiation of dendrite growth. The formation of dendritic branches is found to occur at the expense of island shrinkage. The termination of growth results from the depletion of material surrounding the branches, and the fractal shapes are stable when the branches are fully developed as shown in Figure 2.

The temperature of the environment is found to influence the growth rate of the branches. To quantify the effect of the temperature, we measured the average branch growth rate during annealing (fig. 3). At 30 ^{o}C the rate of growth is found to be 0.15 (± 0.03) μm/s. The growth rate increases almost linearly and displays an interesting

maximum at ~ 45 ^{o}C, before falling to essentially zero at 60 ^{o}C. Further heating led to shrinkage of the dendrite structures with complete disappearance at 85 ^{o}C.

The rates of growth, and shrinkage, of the dendritic branches as a function of temperature can be understood within the framework of a simple theoretical model that takes into account competing processes of: (1) surface-diffusion-mediated molecular aggregation; and (2) thermal desorption of PETN molecules from the aggregated dendrites. Process (1) dominates at temperatures less than 60 ^{o}C, thereby leading to a net growth rate of the branches, while process (2) takes over at higher temperatures, resulting in feature shrinkage and ultimate disappearance. The model is mathematically described as below.

A dendrite with linear dimensions *s* and fractal dimension *f* consists of a total number of molecules given by $N(s) = ks^{f}$, where *k* is a proportionality constant. The rate of molecular addition to this dendrite is given by:

$$\dot{N}_{+} = p_{d} A(s) \nu \exp(-\Delta_{+} / k_{B} T) \ , \qquad (1)$$

where a "dot" represents the time-rate of change (everywhere throughout the text), $\Delta_{+} = \Delta_{gen} + \Delta_{diff}$ is the sum of: (1) activation barrier of the generation of the surface-mobile molecules from the amorphous film surface (Δ_{gen}), and (2) activation barrier of surface diffusion of the mobile species (Δ_{diff}), while *A(s)* contains unknowns like the pre-factor of diffusion constant, pre-factor of surface density of mobile species, etc., but should be relatively insensitive to temperature *T*, which is already expressed through the exponential term. The quantity ν in eq. (1) is an effective vibrational frequency, and p_{d}

is the probability that the diffusing molecule does not desorb from the surface during its diffusion path to the dendrite. This probability is given by $p_d = \exp(-r_d \tau_d)$, where r_d is the rate of desorption (into the vacuum) from the diffusing surface, and τ_d is the average diffusion time. These quantities can be estimated as: $r_d \sim \nu \exp(-\Delta_{des} / k_B T)$ and $\tau_d \sim \frac{\lambda_d^{\,2}}{a^2 \nu} \exp(\Delta_{diff} / k_B T)$, where Δ_{des} is the energy barrier to desorb from the diffusing surface, λ_d is a mean-free path of diffusion, and a is the nearest-neighbor distance on the Si surface, being ~ 0.5 nm.

While $\dot{N}_+$ represents a source term, there is a sink term governed by the thermal desorption of PETN molecules from the dendrite, which is given by the expression $\dot{N}_- = \frac{P_{eq}}{\sqrt{2\pi M k_B T}} \alpha N_{surf}(s)$, where $N_{surf}(s)$ is the number of surface-exposed sites of the dendrite, M and α are the mass and the surface area per PETN molecule, and P_{eq} the equilibrium pressure given by the formula[19]:

$$P_{eq} = \frac{k_B T}{\Lambda^3} \frac{Z_{rot}}{\{Z_{vib}(\nu_{eff})\}^6} \exp(-\Delta E_{sub} / k_B T), \qquad (2)$$

where Z_{rot} and Z_{vib} are rotational and vibrational partition functions of a PETN molecule [20], Λ is the thermal de Broglie wavelength ($\Lambda = h / \sqrt{2\pi M k_B T}$, h being the Planck's constant), ν_{eff} ~ 1.0 x 10^{13} s^{-1} is an affective frequency defined in ref [19] that accurately reproduces PETN vapor pressure, and ΔE_{sub} is the sublimation energy. The

experimentally observed "branch growth rate" is simply the rate of change of *s*. This is given by the equation: $\dot{N}_s = \dot{N}_+ - \dot{N}_-$, which can be simplified to:

$$\dot{s} = s\{C_+(s)\, p_d \nu \exp(-\Delta_+ / k_B T) - C_-(s)\dot{\varphi}_{des}\}, \qquad (3)$$

where $C_+(s) = A(s)/(fN(s))$ and $C_-(s) = N_{surf}(s)/(fN(s))$ are dimensionless quantities assumed insensitive to *T*, and the site desorption rate $\dot{\varphi}_{des}$ is given by:

$$\dot{\varphi}_{des} = \frac{k_B T}{h}\frac{\alpha}{\Lambda^2}\frac{Z_{rot}}{\{Z_{vib}(\nu_{eff})\}^6}\exp(-\Delta E_{sub} / k_B T), \qquad (4)$$

a familiar expression from Transition State Theory. [21]

We now use the above formalism to interpret the observed branch growth rate of Fig. 3 for a fixed size-scale $s \sim 100$ μm (see Fig. 2). From molecular dynamics calculations using the COMPASS force field,[22] we determined the relevant energies (in kcal/mol) as: $\Delta_{gen} \sim 22$, $\Delta_{diff} \sim 2$, $\Delta_{des} \sim 17$, and $\Delta E_{sub} \sim 37$. We also assume all vibrational frequencies to be $\nu \sim \nu_{eff} = 1\text{x}10^{13}$ s^{-1}. From Fig. 2 the diffusion mean free path λ_d appears to be a few tens of microns. The solid curve in Fig. 3 displays the branch growth rate $\dot{s}$ computed by eq. (4) using parameters $\lambda_d \sim 85$ μm, $C_+(s) \sim 58.3$, and $C_-(s) \sim 5.2\text{x}10^{-4}$. The dotted (+) and dashed (-) curves also separately show the contribution of the source (i.e. addition rate by diffusion) and the sink (i.e. reduction rate through evaporation) terms to the overall growth process. The net growth rate is the difference between the (+) and (-) curves. One clearly sees that the maximum at $T \sim 45$ °C occurs solely in the source term. This is because this term involves the product of two functions (see eq. (1)), i.e., the probability p_d that decreases as a function of *T*, and $\exp(-\Delta_+/k_B T)$ that increases as a function of *T*. Below 45 °C the increase in growth rate with temperature is due to faster

diffusion, which outweighs losses due to evaporation of the diffusing species. However, above 45 ^{o}C the rate of evaporation of the diffusing species becomes too significant and leads to a gradual reduction in the growth rate. At the same time, the rate of evaporation from the dendrite surface picks up beyond 45 ^{o}C and continues to increase. There is a crossover of the source and the sink contributions at 60 ^{o}C, leading to zero growth rate at this temperature, and a net shrinking of the dendrite beyond 60 ^{o}C. Fig. 4 displays the experimentally measured branch shrinking rate between temperatures of 60 and 80 ^{o}C. If we use a constant value of the surface fraction $N_{surf}(s)/N(s)$ (which is just f times C$_{-}$(s)) during the whole shrinking process, we get good agreement with the experimental shrinking rates for T up to 70 ^{o}C. However, for higher temperatures we find that the computed shrinking rates are progressively more underestimated. This can be interpreted as more and more sites being surface-exposed at higher temperatures with a concomitant increase in surface fraction (see inset of Fig. 4).

In this work, we demonstrated dendrite growth from thin films of the energetic organic material PETN and quantitatively studied growth and shrinkage rates as a function of temperature. We showed that a simple theoretical model based on surface diffusion, aggregation, and thermal desorption can quantitatively explain the observed data, provided internal molecular degrees of freedom are consistently incorporated in the desorption analysis. This work may aid in understanding growth kinetics and coarsening processes in PETN, and other organic materials. The authors would like to thank finical support from NSF CAREER (CBET-0644832). The work at LLNL was performed under the auspices of the U.S. Department of Energy by Lawrence Livermore National Laboratory under Contract DE-AC52-07NA27344.

Reference

1. L. Granasy, T. Pusztai, T. Borzsonyi, J. A. Warren and J. F. Douglas, Nature Materials **3** (9), 645-650 (2004).
2. F. J. M. Z. Heringdorf, M. C. Reuter and R. M. Tromp, Nature **412** (6846), 517-520 (2001).
3. V. Ferreiro, J. F. Douglas, J. A. Warren and A. Karim, Phys. Rev. E **65** (4), 4 (2002).
4. J. Nittmann, G. Daccord and H. E. Stanley, Nature **314** (6007), 141-144 (1985).
5. T. A. Witten and L. M. Sander, Phys. Rev. Lett. **47** (19), 1400 (1981).
6. P. Meakin, Phys. Rev. Lett. **51** (13), 1119 (1983).
7. P. Jensen, A. L. Barabasi, H. Larralde, S. Havlin and H. E. Stanley, Phys. Rev. E **50** (1), 618-621 (1994).
8. C. M. Feng, H. L. Ge, M. R. Tong, G. X. Ye and Z. K. Jiao, Thin Solid Films **342** (1-2), 30-34 (1999).
9. D. Aurongzeb, E. Washington, M. Basavaraj, J. M. Berg, H. Temkin and M. Holtz, J. Appl. Phys. **100** (11), 114320/114321-114320/114324 (2006).
10. B. Blum, R. C. Salvarezza and A. J. Arvia, J. Vac. Sci. Technol. B **17** (6), 2431-2438 (1999).
11. C. S. Olsen and H. S. Scroggins, J. Pharm. Sci. **73** (9), 1303-1304 (1984).
12. D. A. Knowles, *Chemistry and technology of agrochemical formulations* (Springer, 1998).
13. W. P. King, S. Saxena, B. A. Nelson, B. L. Weeks and R. Pitchimani, Nano Lett. **6** (9), 2145-2149 (2006).
14. The substrates were cleaned by Piranha solution (98% H2SO4 and 30% H2O2 in volume ratios of 3:1) under agitation for 30 min, rinsed with de-ionized water and dried. Caution: piranha solution reacts violently with most organic materials and must be handled with extreme care.
15. G. Zhang, R. Pitchimani and B. L. Weeks, Rev. Sci. Instrum. **79** (9), 096102/096101-096102/096103 (2008).
16. M. Volmer and A. Weber, Z. physik. Chem. **119**, 277-301 (1926).
17. B. I. Kaidymov, Kinet. Katal. **8** (1), 60-65 (1967).
18. G. Zhang and B. L. Weeks, Scanning **30** (3), 228-231 (2008).
19. A. Maiti, L. A. Zepeda-Ruiz, R. H. Gee and A. K. Burnham, J. Phys. Chem. B **111** (51), 14290-14294 (2007).
20. L. A. Zepeda-Ruiz, G. H. Gilmer, A. Maiti, R. H. Gee and A. K. Burnham, J. Cryst. Growth **310** (16), 3812-3819 (2008).
21. G. Hlawacek, P. Puschnig, P. Frank, A. Winkler, C. Ambrosch-Draxl and C. Teichert, Science **321** (5885), 108-111 (2008); S. Glasstone, K. J. Laidler, and H. Eyring, *The Theory of Rate Processes*, McGraw-Hill: New York (1941); R. I. Masel, *Chemical Kinetics and Catalysis*, Wiley-Interscience, New York (2001)
22. S. W. Bunte and H. Sun, J. Phys. Chem. B **104** (11), 2477-2489 (2000).

Figure Captions:

Figure 1: AFM images of PETN films deposited on silicon. The film thicknesses measured by QCM are A) 40.2 nm, B) 70 nm, C) 280.2 nm, D) ~500 nm.

Figure 2: Optical images of PETN deposited on silicon showing dendritic growth at room temperature. A) As deposited PETN; B) Image after 60 minutes; C) 90 minutes; D) after 170 minutes. The scale bar is 100 μm.

Figure 3: Growth rate of dendrite branches as a function of temperature. Circles indicate experimental observations. The solid line represents the theoretical net growth curve; it is a sum of the dotted (+) and dashed (-) curves showing the addition rate by diffusion and the reduction rate through evaporation, respectively.

Figure 4: The experimental measurements (circles) of branch shrinking rate between temperatures of 60 and 80 ^{o}C, along with the corresponding theoretical fit (solid line). (Inset) Temperature-dependent surface fraction $N_{surf}(s)/N(s)$ of molecules used in the theoretical fit.

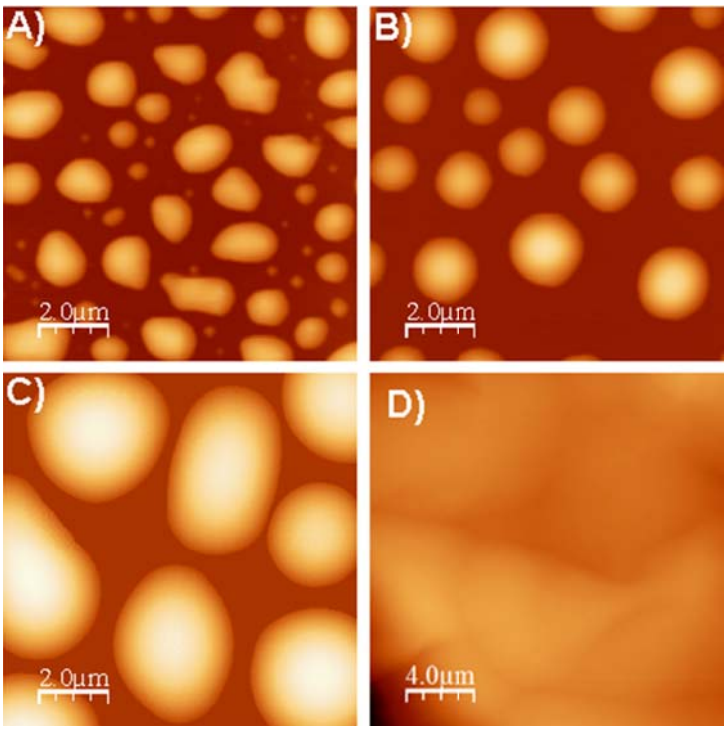

Figure 1

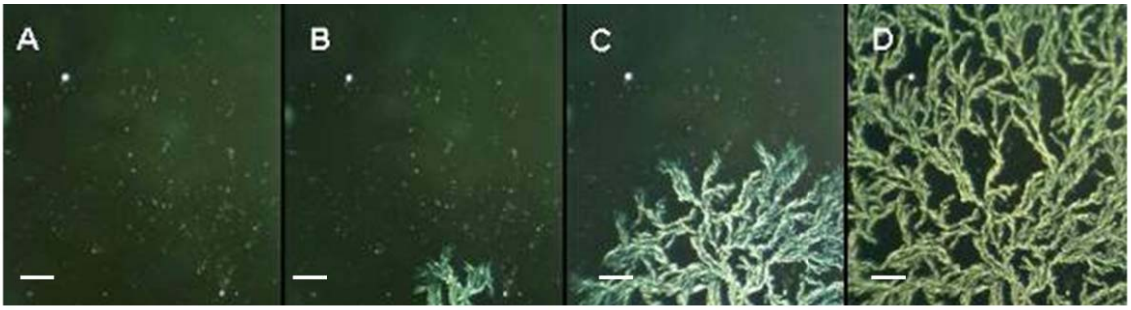

Figure 2

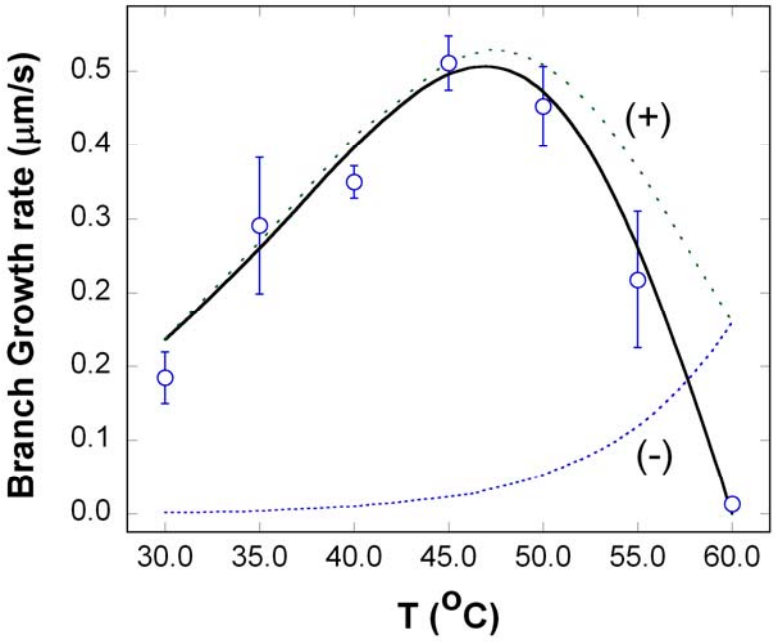

Figure 3

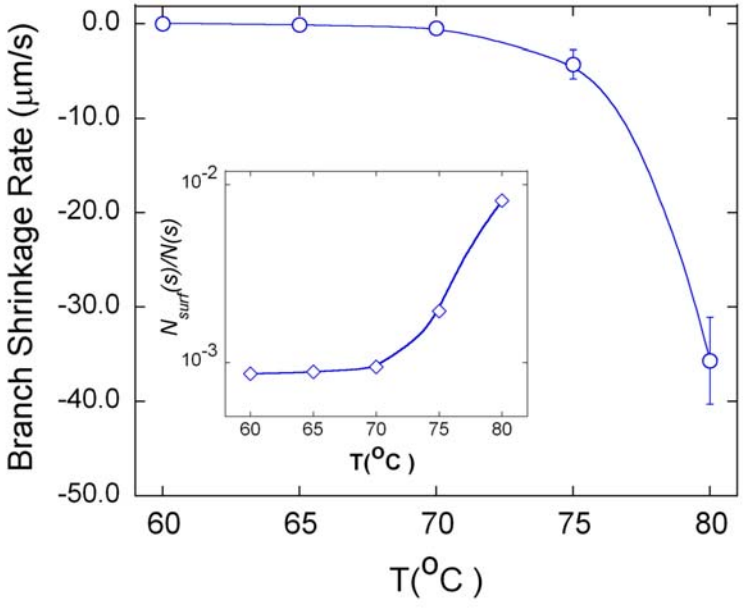

Figure 4